Research Square

Preprints are preliminary reports that have not undergone peer review.
They should not be considered conclusive, used to inform clinical practice,
or referenced by the media as validated information.

Anterior Segment Optical Coherence Tomography Angiography for Differentiating Ocular Surface Squamous Neoplasia from Pterygium

Bayan poormohammad
Tehran University of Medical Sciences
Sanaz Naybandi
Kerman University of Medical Sciences
Seyed Mehdi Marashi
Tehran University of Medical Sciences
Zahra Montazeriani
Tehran University of Medical Sciences
Hamed Ghasemi
Tehran University of Medical Sciences
Ahmad Masoomi
Ahmad.masoomi1990@gmail.com

Tehran University of Medical Sciences

Research Article

Keywords: Ocular surface squamous neoplasia, Pterygium, Anterior segment OCT angiography, Ocular surface vascularization, Vascular patterns, Vessel diameter index

Posted Date: November 3rd, 2026

DOI: https://doi.org/10.21203/rs.3.rs-11165283/v1

License: This work is licensed under a Creative Commons Attribution 4.0 International License.
Read Full License

Additional Declarations: No competing interests reported.

Abstract

Purpose

To compare qualitative and quantitative vascular characteristics on anterior segment optical coherence tomography angiography (AS-OCTA) between ocular surface squamous neoplasia (OSSN) and pterygium and assess its potential for differentiating these lesions.

Methods

In this cross-sectional study, 66 patients (33 with OSSN and 33 with pterygium) were recruited from a tertiary cornea clinic between February 2025 and January 2026. AS-OCTA images were obtained using a commercially available OCTA platform. Conjunctival vascular features were assessed in superficial and deep layers. Two masked specialists independently evaluated qualitative vascular patterns, with adjudication by a third reviewer. Quantitative parameters, including vessel density (VD), vessel length density (VLD), vessel diameter index (VDI), and fractal dimension (FD), were calculated using customized image-processing algorithms. Group comparisons used regression models adjusted for age and sex, with false discovery rate correction.

Results

The OSSN group was significantly older than the pterygium group (61.48 vs. 49.03 years, $P < 0.001$), with no significant difference in sex distribution ($P = 0.76$). Quantitative OCTA parameters were largely comparable between groups, except for significantly lower superficial VDI in OSSN ($P = 0.001$). Qualitative vascular patterns differed significantly, with tortuous, anastomosing, feeder vessels, and flow shadowing more prevalent in OSSN, while linear and tree-like vessels predominated in pterygium (all $P < 0.05$).

Conclusion

AS-OCTA demonstrated distinct qualitative vascular patterns between OSSN and pterygium despite largely similar quantitative metrics. Tortuosity, anastomoses, feeder vessels, and flow shadowing may serve as valuable noninvasive markers for differentiating OSSN from pterygium.

Key Message

What is known

AS-OCTA can visualize vascular abnormalities of ocular surface lesions and may provide noninvasive information useful for distinguishing OSSN from benign lesions.

What is new

- Tortuous, anastomosing, and feeder vessels and flow shadowing were significantly more prevalent in OSSN than in pterygium.
- Superficial vessel diameter index was significantly lower in OSSN than in pterygium.
- Qualitative vascular morphology provided more apparent discriminatory information than most conventional quantitative OCTA parameters in this cohort.

Introduction

Optical coherence tomography angiography (OCTA) is a relatively recent, noninvasive imaging modality that detects vascular flow by capturing motion contrast from erythrocytes. OCTA has been widely used in retinal diseases to evaluate vascular alterations in conditions such as diabetic retinopathy, age-related macular degeneration, and retinal vascular occlusions, providing both qualitative and quantitative assessments of blood flow [1]. Unlike traditional imaging techniques such as fluorescein angiography (FA) and indocyanine green angiography (ICGA), OCTA does not require intravenous dye administration, making it safer and more comfortable for patients while allowing visualization of both superficial and deep vascular layers with depth-resolved imaging [1, 2]. Initially developed for retinal imaging, OCTA has recently gained increasing interest beyond the posterior segment, with expanding applications in anterior segment structures including the conjunctiva, cornea, and iris in healthy eyes [3–5]. Moreover, OCTA has been utilized to assess vascular changes in various ocular surface conditions, including benign and malignant ocular surface lesions [6, 7], iris vessel dilation as a predictive factor for recurrent inflammation in different forms of iritis and neovascularization secondary to proliferative diabetic retinopathy [8], conjunctival vascular alterations in thyroid eye disease [9], evaluation of surgical outcomes such as conjunctival autograft vascularization following pterygium surgery [10], and as a prognostic tool for predicting complications after chemical injuries. [11]

Ocular surface squamous neoplasia (OSSN) represents the most common malignant lesion of the ocular surface, encompassing a spectrum from conjunctival and corneal intraepithelial neoplasia to invasive squamous cell carcinoma.[12] Ultraviolet light exposure and human papillomavirus (HPV) infection are among the primary risk factors.[13] Historically, diagnosis relied on clinical examination and, in suspected cases, was followed by histopathologic confirmation to differentiate OSSN from more benign lesions such as pterygium. With advances in anterior segment OCT and OCTA, the need for invasive diagnostic procedures has been substantially reduced. [13, 14]

Recent studies indicate that OCTA may further enhance the diagnostic capability for OSSN by visualizing abnormal tumor-associated vascular networks. [15] Quantitative parameters, including vessel density (VD), vessel diameter index (VDI), and vascular length density (VLD), have shown potential in assessing tumor activity and monitoring response to topical immunotherapy. [16]

In this study, we compared OCTA-derived vascular characteristics of OSSN and pterygium. By evaluating differences in vascular patterns and quantitative metrics between these two entities, we sought to

determine whether OCTA can serve as a reliable, noninvasive tool to aid in distinguishing OSSN from pterygium in clinical practice.

Methods

Methods

Study Design and Participants

This cross-sectional study was conducted between February 2025 and January 2026 in the Cornea Department of Farabi Eye Hospital. The study adhered to the tenets of the Declaration of Helsinki and was approved by the Institutional Review Board of Tehran University of Medical Sciences (ethics code: IR.TUMS.FARABIH.REC.1404.010). Written informed consent was obtained from all participants before clinical imaging.

Patients were consecutively recruited from the cornea clinic during the study period. A total of 66 patients were included, comprising 33 patients with ocular surface squamous neoplasia (OSSN) and 33 with pterygium. The diagnosis was established clinically by a cornea fellowship-trained specialist. In cases of diagnostic uncertainty, impression cytology or excisional biopsy was performed for confirmation.

Patients were excluded if they had ocular or systemic conditions that could affect ocular surface vascularization, including diabetes mellitus, previous ocular surgery, previous intravitreal bevacizumab injection, use of topical antiglaucoma medications, contact lens wear, or severe dry eye. Eyes with poor-quality OCTA images or slit-lamp photographs that were unsuitable for analysis were also excluded.

AS-OCTA Acquisition

All participants underwent anterior segment optical coherence tomography angiography (AS-OCTA) and slit-lamp photography. Imaging was performed using the AngioVue OCTA system (Optovue, Inc., Fremont, CA, USA), primarily using the AngioRetina mode designed for retinal imaging. The system operates at a central wavelength of 840 nm with a bandwidth of 22 nm and an acquisition rate of 70,000 A-scans per second, with an axial resolution of approximately 5 μm in tissue.

A 3 × 3-mm scan pattern with 304 × 304 A-scans was acquired over approximately 3–4 seconds. Two consecutive B-scans were obtained at each position to distinguish static tissue from blood-flow signals. Blood flow was detected by comparing sequential images using the split-spectrum amplitude-decorrelation angiography (SSADA) algorithm with motion-correction techniques.

AS-OCTA images were acquired at two predefined depths relative to the conjunctival epithelium:

1. **Superficial layer**: from the conjunctival epithelium to a depth of 200 μm.
2. **Deep layer**: deeper than 200 μm from the conjunctival epithelium.

Image Processing and Quantitative Analysis

OCTA images were analyzed using MATLAB 2021b (MathWorks, Natick, MA, USA). A predefined region of interest (ROI) was manually delineated by an experienced grader who was masked to the clinical diagnosis. To improve vessel contrast and reduce image-processing artifacts, contrast-limited adaptive histogram equalization and median filtering were applied to the grayscale images.

The Otsu thresholding method was subsequently used to binarize the images and identify vascular structures by minimizing the intra-class variance between foreground and background pixels. The resulting segmentation was reviewed and manually corrected by the same experienced grader when necessary.

Quantitative vascular parameters included vessel density (VD), vessel length density (VLD), vessel diameter index (VDI), and fractal dimension (FD).

Vessel density (VD) was defined as the proportion of the ROI occupied by perfused vessels:

VD = total vessel area / total ROI area.

Vessel length density (VLD) was defined as the cumulative length of detected vessels normalized to the ROI area:

VLD = total vessel length / total ROI area.

Vessel diameter index (VDI) was calculated as an estimate of mean vessel caliber based on the ratio of vessel area to total vessel length:

VDI = total vessel area / total vessel length.

Fractal dimension (FD) was used as a measure of vascular network complexity. FD was calculated using a box-counting algorithm applied to the skeletonized vascular image, with higher values indicating greater branching complexity.

Qualitative Vascular Assessment

Qualitative vascular characteristics were assessed independently by two specialists who were masked to the clinical diagnosis. Disagreements were resolved by a third reviewer.

Vascular morphology was classified into the following patterns: linear (straight), looped (arcade), tree-like (arborizing), anastomosing, tortuous, feeder, corkscrew (coiled), chaotic (disorganized), and flow-

shadowing patterns.[Fig. 1]

Statistical Analysis

All statistical analyses were performed using IBM SPSS Statistics version 28 (IBM Corp., Armonk, NY, USA). Continuous variables were summarized as mean ± standard deviation (SD) or median and range, as appropriate. Categorical variables were summarized as frequencies and percentages.

Baseline characteristics were compared between the OSSN and pterygium groups using independent-samples t-tests for continuous variables and χ^2 tests or Fisher's exact tests for categorical variables, as appropriate.

For quantitative OCTA parameters, generalized linear models were used to estimate differences between groups after adjustment for age and sex. Results were reported as adjusted regression coefficients with 95% confidence intervals (CIs) based on Wald statistics.

For binary qualitative vascular patterns, logistic regression models with a binomial distribution and logit link were used to estimate the association between lesion type and each vascular pattern, adjusting for age and sex. Results were reported as adjusted odds ratios (ORs) with 95% CIs.

The Benjamini–Hochberg false discovery rate (FDR) procedure was applied to account for multiple comparisons. All statistical tests were two-sided, and a P value < 0.05 was considered statistically significant.

RESULTS

All 66 eligible patients identified during the study period were included; no patients were excluded due to incomplete imaging. A total of 33 patients with pterygium and 33 patients with OSSN were included in this study. The mean age in the OSSN group was 61.48 years (range: 31 to 93 years), and in the pterygium group, it was 49.03 years (range: 24 to 72 years). In the OSSN group, 75.8% were men and 24.2% were women, while in the pterygium group, 78.8% were men and 21.2% were women. The OSSN group was significantly older than the pterygium group (P < 0.001), while sex distribution did not differ significantly between the two groups (P = 0.769).

Quantitative parameters—VD, VLD, VDI, and fractal dimension (FD)—were evaluated in both the superficial and deep layers. In the deep layer, the mean VD was 0.31 in OSSN and 0.33 in pterygium(P = 0.28). The mean VLD was 0.16 mm/mm² in OSSN and 0.17 mm/mm² in pterygium (P = 0.40). The mean VDI was 1.92 μm in OSSN and 1.97 μm in pterygium(P = 0.19).

In the superficial layer, the mean VD was 0.32 in OSSN and 0.35 in pterygium (p = 0.15), the mean VLD was 0.17 mm/mm² in both groups (p = 0.87), and the mean VDI was 1.91 μm in OSSN and 2.05 μm in pterygium (p < 0.001). The significantly lower superficial VDI in OSSN indicates a predominance of smaller-caliber superficial vessels compared with pterygium.

The mean fractal dimension in both superficial and deep layers was 1.84 in both groups (P = 0.52, 0.90 respectively), indicating similar vascular branching complexity. Among the quantitative parameters, only superficial-layer VDI differed significantly between OSSN and pterygium .[Table 1]

Table 1
Quantitative OCTA vascular parameters in OSSN and pterygium

OCTA parameter	Layer	OSSN, mean ± SD	Pterygium, mean ± SD	Mean difference	95% CI	P value
Vessel density (VD)	Deep	0.314 ± 0.080	0.336 ± 0.082	−0.022	−0.062 to 0.018	0.281
Vessel length density (VLD), mm/mm²	Deep	0.162 ± 0.037	0.170 ± 0.040	−0.008	−0.027 to 0.011	0.404
Vessel diameter index (VDI), μm	Deep	1.928 ± 0.140	1.970 ± 0.119	−0.042	−0.106 to 0.022	0.195
Fractal dimension (FD)	Deep	1.849 ± 0.033	1.848 ± 0.031	0.001	−0.015 to 0.017	0.904
Vessel density (VD)	Superficial	0.327 ± 0.064	0.354 ± 0.086	−0.027	−0.064 to 0.010	0.152
Vessel length density (VLD), mm/mm²	Superficial	0.171 ± 0.033	0.172 ± 0.040	−0.001	−0.020 to 0.017	0.874
Vessel diameter index (VDI), μm	Superficial	1.917 ± 0.145	2.054 ± 0.154	−0.137	−0.210 to − 0.063	< 0.001
Fractal dimension (FD)	Superficial	1.848 ± 0.034	1.843 ± 0.034	0.005	−0.011 to 0.022	0.523

Abbreviations: CI, confidence interval; FD, fractal dimension; OCTA, optical coherence tomography angiography; OSSN, ocular surface squamous neoplasia; SD, standard deviation; VD, vessel density; VDI, vessel diameter index; VLD, vessel length density.

ROC curve analysis showed that superficial VDI had moderate discriminatory ability to differentiate Ocular Surface Squamous Neoplasia (OSSN) from Pterygium, with an area under the curve (AUC) of 0.73 (95% CI: 0.61–0.85). The optimal cutoff value was 1.99 μm, providing 63% sensitivity and 69% specificity. [Fig. 2]

Regarding qualitative vascular patterns, significant differences were observed between the two groups for linear (straight) vessels ($p < 0.001$), tree-like (arborizing) vessels ($p < 0.001$), looped (arcade) vessels ($p = 0.001$), tortuous vessels ($p = 0.003$), anastomosing vessels ($p < 0.001$), feeder vessels ($p = 0.003$), and flow shadowing ($p < 0.001$). No significant differences were found for disorganized (chaotic) vasculature ($p = 0.056$) or corkscrew (coiled) vessels ($p = 0.769$) (Table 2). These findings indicate

distinct vascular architectural patterns between OSSN and pterygium, particularly in vessel morphology and connectivity.

Table 2. Qualitative vascular patterns in OSSN and pterygium

Vascular feature	OSSN, n (%)	Pterygium, n (%)	P value
Linear vessels	**1 (3.0)**	**20 (60.6)**	**<0.001**
Tree-like (arborizing) vessels	**5 (15.2)**	**23 (69.7)**	**<0.001**
Looped (arcade) vessels	**1 (3.0)**	**11 (33.3)**	**0.001**
Tortuous vessels	**24 (72.7)**	**12 (36.4)**	**0.003**
Disorganized (chaotic) vasculature	**9 (27.3)**	**3 (9.1)**	**0.056**
Corkscrew (coiled) vessels	**7 (21.2)**	**8 (24.2)**	**0.769**
Anastomosing vessels	**20 (60.6)**	**4 (12.1)**	**<0.001**
Feeder vessels	**19 (57.6)**	**7 (21.2)**	**0.003**
Flow shadowing	**17 (51.5)**	**1 (3.0)**	**<0.001**

The most common patterns in pterygium were linear and tree-like vessels (60.6% and 69.7%, respectively), consistent with organized fibrovascular growth typical of degenerative conjunctival lesions. In contrast, tortuous vessels were the predominant pattern in OSSN (72.7%), suggesting irregular neoplastic angiogenesis. [Table 2]

Quantitative and qualitative parameters were further analyzed using ANCOVA adjusted for age and sex. For quantitative variables, the mean differences in the OSSN group compared with the pterygium group were as follows: in the deep layer, VD − 0.011 ($p = 0.605$), VLD − 0.004 ($p = 0.073$), VDI − 0.025 ($p = 0.465$), and fractal dimension + 0.002 ($p = 0.810$). In the superficial layer, the differences were VD − 0.026 ($p = 0.203$), VLD − 0.020 ($p = 0.866$), and fractal dimension + 0.003 ($p = 0.750$). Only VDI in the superficial layer showed a significant difference (− 0.129, $p = 0.001$), confirming reduced superficial vessel caliber as an independent distinguishing feature of OSSN. [Fig. 3]

For qualitative parameters, logistic regression adjusted for age and sex demonstrated significant associations between group and several vascular patterns: linear vessels (OR = 0.006, $p < 0.001$), tree-like vessels (OR = 0.057, $p < 0.001$), looped vessels (OR = 0.052, $p = 0.011$), tortuous vessels (OR = 6.389, $p = 0.003$), anastomosing vessels (OR = 11.158, $p = 0.001$), feeder vessels (OR = 4.517, $p = 0.013$), and flow shadowing (OR = 128.558, $p < 0.001$). These results indicate that tortuous, anastomosing, and feeder vessels as well as flow shadowing, were strongly associated with OSSN, whereas linear and arborizing vessels were more characteristic of pterygium. Chaotic vessels (OR = 4.161, $p = 0.074$) and corkscrew vessels (OR = 0.792, $p = 0.730$) did not differ significantly between groups. [Fig. 4]

Overall, these results suggest that while quantitative OCTA metrics are largely similar between OSSN and pterygium, superficial vessel caliber and qualitative vascular patterns differ significantly, providing potential noninvasive biomarkers for differentiation

DISCUSSION

Tumor expansion beyond a few millimeters requires sustained pathological angiogenesis to supply oxygen and nutrients while facilitating metabolic waste removal. This process is primarily driven by hypoxia-induced upregulation of angiogenic mediators, particularly vascular endothelial growth factor (VEGF), and is characterized by structurally abnormal, tortuous, and inefficient vascular networks. [17] In ocular surface squamous neoplasia (OSSN), angiogenesis reflects the fundamental mechanisms of tumor biology. Ultraviolet-induced DNA damage, together with viral oncogenesis and dysregulation of angiogenic signaling pathways, promotes neoplastic transformation and upregulation of VEGF expression. These molecular alterations stimulate the formation of immature, tortuous feeder vessels and a disorganized intratumoral microvascular network, which are characteristic features of malignant angiogenesis. [18, 19] In contrast, although pterygium is now recognized as an active fibrovascular proliferative disorder rather than a purely degenerative lesion, its angiogenesis is predominantly reactive and more structurally organized. Chronic ultraviolet exposure, oxidative stress, and inflammatory mediators promote subepithelial neovascularization and fibrovascular proliferation. Consequently, pterygium typically demonstrates organized linear or arborizing vascular networks, whereas OSSN exhibits more chaotic, tortuous, and irregular vascular patterns characteristic of malignant angiogenesis. [20, 21]

One of the most notable findings of the present study was the significantly lower superficial vessel diameter index (VDI) in OSSN compared with pterygium, suggesting that superficial vessel caliber may serve as a useful imaging biomarker for differentiating these lesions. Several mechanisms may explain this observation. First, tumor angiogenesis typically produces numerous fine, tortuous, and highly branched microvessels, which also may predominantly generate immature capillary-sized vessels rather than dilated mature vessels [22] whereas pterygium contains well-developed fibrovascular tissue with larger and more organized superficial vascular bundles. [23] These fundamental differences in vascular architecture may partly account for the higher superficial VDI observed in pterygium. Second, epithelial thickening and subepithelial tumor growth in OSSN [12] may compress superficial microvessels, reducing their apparent caliber. Third, previous OCTA studies have shown that vascular density in OSSN is greatest within the subepithelial tissue beneath the tumor, indicating that a substantial proportion of tumor-associated vasculature is located in deeper tissue planes.[15] This distribution may partly explain the lower superficial VDI observed in our study, as superficial OCTA measurements may not fully capture the deeper vascular component of OSSN. Finally, pterygium is characterized by chronic inflammation and fibrovascular proliferation with increased expression of proangiogenic mediators, including VEGF, which promotes vascular remodeling, vasodilation, and enlargement of superficial conjunctival vessels.

[24, 25] Collectively, these biological differences in vascular remodeling may explain the significantly higher superficial VDI observed in pterygium in our cohort.

Consistent with this finding, ROC analysis demonstrated that a superficial VDI cutoff of approximately 2.0 yielded an AUC of 0.73, with a sensitivity of 63% and specificity of 69%, suggesting that superficial vessel caliber may serve as a useful adjunctive biomarker for the non-invasive differentiation of OSSN from pterygium. [Fig. 2] Although the diagnostic performance was moderate, this threshold may provide a practical adjunct to qualitative vascular assessment when differentiating OSSN from pterygium in routine clinical practice.

In this study, we compared vascular characteristics of OSSN and pterygium using AS-OCTA. While quantitative vascular parameters, except VDI in the superficial layer, did not significantly differ between the two groups, distinct qualitative vascular patterns were observed. These findings suggest that AS-OCTA may offer clinically meaningful, noninvasive differentiation of OSSN from pterygium, primarily through qualitative vascular profiling.

Several previous studies have emphasized the role of AS-OCTA in characterizing vascular abnormalities in ocular surface malignancies. Lee et al. reported that malignant lesions tend to exhibit larger peri-lesional vessel diameters and deeper peri-lesional vasculature, consistent with feeder vessel formation and tumor-driven angiogenesis.[7] In our study, although mean quantitative vessel diameter indices were largely comparable between OSSN and pterygium, the qualitative presence of feeder vessels and flow shadowing was significantly higher in OSSN, supporting the observation that malignant lesions exhibit distinctive angiogenic behavior not fully captured by averaged quantitative metrics alone.

Similarly, Liu et al. performed detailed OCTA analyses of vascular morphology surrounding OSSN lesions and demonstrated increased sub-epithelial vascular density and aberrant vessel architecture compared with adjacent normal conjunctiva. Their findings highlight the capacity of OCTA to visualize abnormal tumor-associated vascular networks, characterized by irregular branching and atypical vessel morphology.[15] In contrast to their results, our study did not identify significant differences in overall vessel density or fractal dimension between OSSN and pterygium. Notably, Liu et al. compared OSSN with normal conjunctiva, whereas our study compared OSSN with another fibrovascular pathology, pterygium. Nevertheless, the higher prevalence of tortuous and anastomosing vessels in OSSN in our cohort aligns with Liu et al.'s description of aberrant neoplastic vasculature and underscores the importance of qualitative vascular assessment.

A case report done by Nampei et al. described characteristic vascular patterns in OSSN and other ocular surface tumors using AS-OCTA, such as "zigzag" meandering vessels in OSSN versus straighter vessels in pterygium, which can aid differentiation of these lesions. [26] Similarly, in our study, we identified distinct vascular patterns that may help differentiate pterygium from OSSN.

Longitudinal evaluation of tumor vasculature has further supported the dynamic nature of OSSN angiogenesis. Theotoka et al. demonstrated that longitudinal OCTA imaging could detect changes in

vessel area density and vascular complexity following treatment, reinforcing the concept that tumor angiogenesis is not static and can be monitored non-invasively over time. These findings suggest a potential role for OCTA not only in diagnosis but also in treatment monitoring.[27] Although our study was cross-sectional and did not assess longitudinal changes, we observed marked differences in qualitative vascular patterns between OSSN and pterygium at baseline.

Consistent with this therapeutic perspective, Ghasemi et al. evaluated OCTA parameters during topical treatment of OSSN and reported significant changes in superficial vessel density and superficial vessel diameter index, while deep vascular parameters and vessel length density remained unchanged. These results suggest that superficial vascular layers may be more responsive to topical chemotherapy, reflecting regression of tumor-associated angiogenesis at the epithelial and subepithelial levels.[16] In our study, a similar pattern was observed in that only superficial VDI differed significantly between OSSN and pterygium after adjustment, while deep-layer quantitative parameters showed no significant differences. These findings support the hypothesis that superficial vascular alterations are more sensitive markers of neoplastic activity, whereas deeper vessels may be less affected or more prone to shadowing artifacts and segmentation limitations.

Interestingly, our findings align with more recent reports suggesting that OCTA-derived quantitative parameters may be limited by projection artifacts, shadowing, and the inherently superficial nature of many OSSN lesions. Instead, qualitative vessel morphology—such as tortuosity, feeder vessels, and anastomoses—has been increasingly recognized as a more reliable indicator of neoplastic angiogenesis. In the present study, tortuous, anastomosing, and feeder vessels were significantly more prevalent in OSSN, consistent with tumor-driven vascular remodeling. Conversely, pterygium predominantly demonstrated linear (straight) and arborizing vessels, reflecting its fibrovascular, non-neoplastic growth pattern described in earlier histopathologic and angiographic studies.

Although OSSN and pterygium may appear clinically similar, their vascular physiology differs considerably. OSSN typically exhibits chaotic and metabolically active angiogenesis; this was reflected in our higher prevalence of tortuous, anastomosing, and feeder vessels, as well as the markedly increased odds of flow shadowing in OSSN. Flow shadowing may be particularly useful clinically, as it suggests dense cellular proliferation or keratinization—features frequently observed in OSSN but not in pterygium.

The lack of significant differences in quantitative OCTA metrics may indicate that vessel density and other quantitative OCTA parameters alone may be insufficient to distinguish these lesions, particularly when superficial and deep vasculature overlap or when lesions produce shadowing artifacts. Additionally, current OCTA technology may be unable to fully visualize intratumoral vascularity. Thus, OCTA-derived qualitative vascular signatures may offer greater diagnostic value in a real-world clinical setting. Incorporating such patterns into routine evaluation could enhance the non-invasive detection of OSSN, reducing the need for diagnostic biopsies in equivocal cases.

Study Limitations

This study has several limitations. First, it was conducted at a single tertiary center, which may limit generalizability. Second, OCTA images were obtained using a retina-designated system, which may not provide optimal imaging depth, resolution, or segmentation accuracy for ocular surface tissue. [28] Third, shadowing artifacts and variations in lesion thickness could have influenced quantitative measurements, potentially masking subtle differences between the two groups. Fourth, we did not correlate OCTA findings with histopathologic vascular analysis, which could have strengthened interpretation of the qualitative vascular features.

Future Directions

Future research should focus on prospective studies using dedicated anterior segment OCTA devices that offer improved segmentation, higher resolution, and better suppression of shadowing artifacts. Incorporating automated machine-learning–based vascular pattern recognition may further enhance diagnostic accuracy and allow development of standardized OCTA criteria for OSSN.

Conclusion

AS-OCTA demonstrated distinct qualitative vascular differences between OSSN and pterygium despite overall similarity in quantitative vascular metrics. Features such as tortuous, anastomosing, and feeder vessels, as well as pronounced flow shadowing, are strongly associated with OSSN and may serve as valuable noninvasive indicators to aid in differentiating neoplastic from benign ocular surface lesions. With further technological refinement and validation, AS-OCTA may become an important adjunct in the diagnostic algorithm for ocular surface tumors.

Declarations

This study received no specific funding.

Ethics approval:

This study was approved by the Ethics Committee of Farabi Eye Hospital, Tehran University of Medical Sciences (IR.TUMS.FARABIH.REC.1404.010) and was conducted in accordance with the Declaration of Helsinki.

Consent to participate:

Written informed consent was obtained from all participants prior to enrollment in the study.

Author Contribution

Concept and Design, Definition of intellectual content, Manuscript editing and manuscript review : Hamed Ghasemi ,MD . Ahmad Masoomi, MDLiterature search, Clinical studies, Experimental studies, Data analysis, Statistical analysis, Manuscript editing and manuscript review: Bayan Poormohammad ,

MD Manuscript preparation, Manuscript editing and manuscript review: Sanaz Naybandi, MD Data acquisition: Zahra Montazeriani. Seyed Mehdi Marashi , MD

References

1. Jia Y, Hormel TT, Hwang TS, Wu AL, Liang GB, Guo Y, Wei X, Ni S, Jian Y, Campbell JP, Bailey ST, Morrison JC, Huang D, Widefield OCT (2025) angiography. Prog Retin Eye Res. ;107:101378. 10.1016/j.preteyeres.2025.101378. Epub 2025 Jun 13. Erratum in: Prog Retin Eye Res. 2025;109:101408. doi: 10.1016/j.preteyeres.2025.101408. PMID: 40517946; PMCID: PMC12342419
2. Spaide RF, Klancnik JM Jr, Cooney MJ (2015) Retinal vascular layers imaged by fluorescein angiography and optical coherence tomography angiography. JAMA Ophthalmol. ;133(1):45–50. 10.1001/jamaophthalmol.2014.3616. PMID: 25317632
3. Ang M, Sim DA, Keane PA, Sng CC, Egan CA, Tufail A, Wilkins MR (2015) Optical Coherence Tomography Angiography for Anterior Segment Vasculature Imaging. Ophthalmology 122(9):1740–1747. 10.1016/j.ophtha.2015.05.017. Epub 2015 Jun 16. PMID: 26088621
4. Akagi T, Uji A, Huang AS, Weinreb RN, Yamada T, Miyata M, Kameda T, Ikeda HO, Tsujikawa A (2018) Conjunctival and Intrascleral Vasculatures Assessed Using Anterior Segment Optical Coherence Tomography Angiography in Normal Eyes. Am J Ophthalmol 196:1–9 Epub 2018 Aug 9. PMID: 30099035; PMCID: PMC6284828
5. Kiseleva TN, Saakyan SV, Makukhina VV, Lugovkina KV, Milash SV, Musova NF, Zharov AA (2022) Vozmozhnosti opticheskoi kogerentnoi tomografii v angiorezhime v otsenke angioarkhitektoniki konyunktivy v norme i pri patologii [Use of optical coherence tomography angiography in assessment in conjunctival vascular architecture in health and pathology]. Vestn Oftalmol. ;138(6):32–42. Russian. 10.17116/oftalma202213806132. PMID: 36573946
6. Binotti WW, Mills H, Nosé RM, Wu HK, Duker JS, Hamrah P (2021) Anterior segment optical coherence tomography angiography in the assessment of ocular surface lesions. Ocul Surf 22:86–93. 10.1016/j.jtos.2021.07.009. Epub 2021 Jul 30. PMID: 34333154; PMCID: PMC11583202
7. Lee BJH, Tey KY, Cheong EZK, Wong QY, Chua CSQ, Ang M (2024) Anterior Segment Optical Coherence Tomography Angiography: A Review of Applications for the Cornea and Ocular Surface. Med (Kaunas) 60(10):1597. 10.3390/medicina60101597. PMID: 39459384; PMCID: PMC11509466
8. Pichi F, Roberts P, Neri P (2019) The broad spectrum of application of optical coherence tomography angiography to the anterior segment of the eye in inflammatory conditions: a review of the literature. J Ophthalmic Inflamm Infect 9(1):18. 10.1186/s12348-019-0184-9. PMID: 31485882; PMCID: PMC6726732
9. Masoumi A, Afshar P, Fakhredin H, Ghanbari H, Montazeri F, Aghajani A, Montazeriani Z, Pasyar P, Zeidabadinejad H, Bijani FM, Rafizadeh SM (2025) Quantifying anterior segment vascular changes in thyroid eye disease using optical coherence tomography angiography. BMC Med Imaging 25(1):85. 10.1186/s12880-025-01627-y. PMID: 40069673; PMCID: PMC11899867

10. Masoumi A, Esfandiari A, Khalili A, Latifi G, Ghanbari H, Jafari B, Montazeriani Z, Rahimi M, Ghafarian S (2025) Assessment of conjunctival autograft reperfusion after pterygium surgery by optical coherence tomography angiography (OCT-A). Microvasc Res 157:104734 Epub 2024 Aug 31. PMID: 39218033
11. Samadi M, Ghanbari H, Ghasemi H, Soltani G, Rezaei A, Montazeriani Z, Atighechian M, Masoumi A, Soleimani M (2025) The role of anterior segment optical coherence tomography angiography in predicting outcomes of acute ocular burns. Burns. ;51(7):107604. 10.1016/j.burns.2025.107604. Epub 2025 Jul 3. PMID: 40674847
12. Sun Y, Hua R (2019) Ocular surface squamous neoplasia: angiographic characteristics and response to subconjunctival/perilesional 5-fluorouracil injections. Drug Des Devel Ther 13:1323–1334. 10.2147/DDDT.S191161. PMID: 31118569; PMCID: PMC6503196
13. Höllhumer R, Williams S, Michelow P (2021) Ocular surface squamous neoplasia: management and outcomes. Eye (Lond) 35(6):1562–1573. 10.1038/s41433-021-01422-3. Epub 2021 Feb 9. PMID: 33564137; PMCID: PMC8169825
14. Davila JR, Mruthyunjaya P Updates in imaging in ocular oncology. F1000Res. 2019;8:F1000 Faculty Rev-1706. 10.12688/f1000research.19979.1. PMID: 31602297; PMCID: PMC6774056.
15. Liu Z, Karp CL, Galor A, Al Bayyat GJ, Jiang H, Wang J (2020) Role of optical coherence tomography angiography in the characterization of vascular network patterns of ocular surface squamous neoplasia. Ocul Surf 18(4):926–935. 10.1016/j.jtos.2020.03.009. Epub 2020 Apr 25. PMID: 32344147; PMCID: PMC9449867
16. Ghanbari H, Masoumi A, Samadi M, Naghshtabrizi N, Aminizade M, Montazeriani Z, Khodaparast M, Montazeri F, Ghassemi H (2025) Optical coherence tomography angiography in evaluating the response of ocular surface squamous neoplasia to topical immunotherapy. Graefes Arch Clin Exp Ophthalmol. Nov 24. 10.1007/s00417-025-07041-y. Epub ahead of print. PMID: 41284036
17. Steger B (2021) Ocular surface angiography: from neovessels to neoplasia. BMJ Open Ophthalmol 6(1):e000829. 10.1136/bmjophth-2021-000829. PMID: 34485703; PMCID: PMC8378387
18. Gichuhi S, Ohnuma S, Sagoo MS, Burton MJ (2014) Pathophysiology of ocular surface squamous neoplasia. Exp Eye Res 129:172–182. 10.1016/j.exer.2014.10.015. Epub 2014 Oct 18. PMID: 25447808; PMCID: PMC4726664
19. Sobczyńska-Rak A, Żylińska B, Nowicka B, Rak E, Rzepka T (2025) Role and Mechanisms of Angiogenesis in Tumours. Biology 14(7):756
20. Livezeanu C, Crăiţoiu MM, Mănescu R, Mocanu C, Crăiţoiu S (2011) Angiogenesis in the pathogenesis of pterygium. Rom J Morphol Embryol 52(3):837–844 PMID: 21892527
21. Zhao F, Cai S, Huang Z, Ding P, Du C (2020) Optical Coherence Tomography Angiography in Pinguecula and Pterygium. Cornea. ;39(1):99–103. 10.1097/ICO.0000000000002114. PMID: 31436638
22. Jain RK (2001) Normalizing tumor vasculature with anti-angiogenic therapy: a new paradigm for combination therapy. Nat Med. ;7(9):987-9. 10.1038/nm0901-987. PMID: 11533692

23. Marcovich AL, Morad Y, Sandbank J, Huszar M, Rosner M, Pollack A, Herbert M, Bar-Dayan Y (2002) Angiogenesis in pterygium: morphometric and immunohistochemical study. Curr Eye Res. ;25(1):17–22. 10.1076/ceyr.25.1.17.9959. PMID: 12518239
24. Aspiotis M, Tsanou E, Gorezis S, Ioachim E, Skyrlas A, Stefaniotou M, Malamou-Mitsi V (2007) Angiogenesis in pterygium: study of microvessel density, vascular endothelial growth factor, and thrombospondin-1. Eye (Lond) 21(8):1095–1101. 10.1038/sj.eye.6702495. Epub 2006 Jun 23. PMID: 16823458
25. Shahraki T, Arabi A, Feizi S (2021) Pterygium: an update on pathophysiology, clinical features, and management. Ther Adv Ophthalmol 13:25158414211020152. 10.1177/25158414211020152. PMID: 34104871; PMCID: PMC8170279
26. Nampei K, Oie Y, Kiritoshi S, Morota M, Satoh S, Kawasaki S, Nishida K (2020) Comparison of ocular surface squamous neoplasia and pterygium using anterior segment optical coherence tomography angiography. Am J Ophthalmol Case Rep 20:100902 PMID: 32995664; PMCID: PMC7502819
27. Theotoka D, Liu Z, Wall S, Galor A, Al Bayyat GJ, Feuer W, Jianhua W, Karp CL (2022) Optical coherence tomography angiography in the evaluation of vascular patterns of ocular surface squamous neoplasia during topical medical treatment. Ocul Surf 25:8–18 Epub 2022 Mar 29. PMID: 35358712; PMCID: PMC9378455
28. Lee WD, Devarajan K, Chua J, Schmetterer L, Mehta JS, Ang M (2019) Optical coherence tomography angiography for the anterior segment. Eye Vis (Lond) 6:4. 10.1186/s40662-019-0129-2. PMID: 30775387; PMCID: PMC6357412

Figures

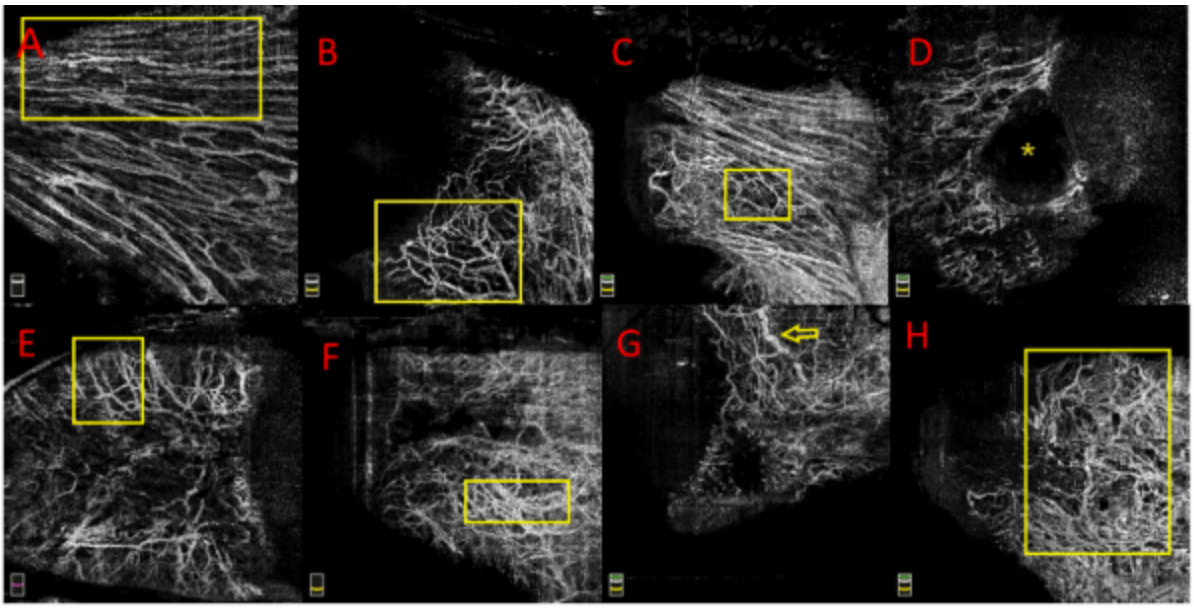


Figure 1

Superficial-layer anterior segment OCTA images of pterygium demonstrating predominantly linear (straight),parallel-oriented vessels within the subepithelial fibrovascular tissue, reflecting organized, non-neoplastic angiogenesis(A), arborizing (tree-like) vascular branching within the superficial conjunctival network(B), looped (arcade) vessels, representing organized subepithelial vascular architecture(C). Superficial-layer anterior segment OCTA images of OSSN demonstrating a central flow shadowing (yellow star) surrounded by disorganized (chaotic) vasculature, consistent with neoplastic angiogenesis(D), anastomosing vessels forming irregular peri-tumoral vascular networks(E), corkscrew (coiled) vessels, reflecting abnormal tumor-associated vascular remodeling(F), a prominent feeder vessel(arrow) supplying the neoplastic lesion(G), markedly tortuous vessels, a characteristic feature of malignant angiogenesis(H).

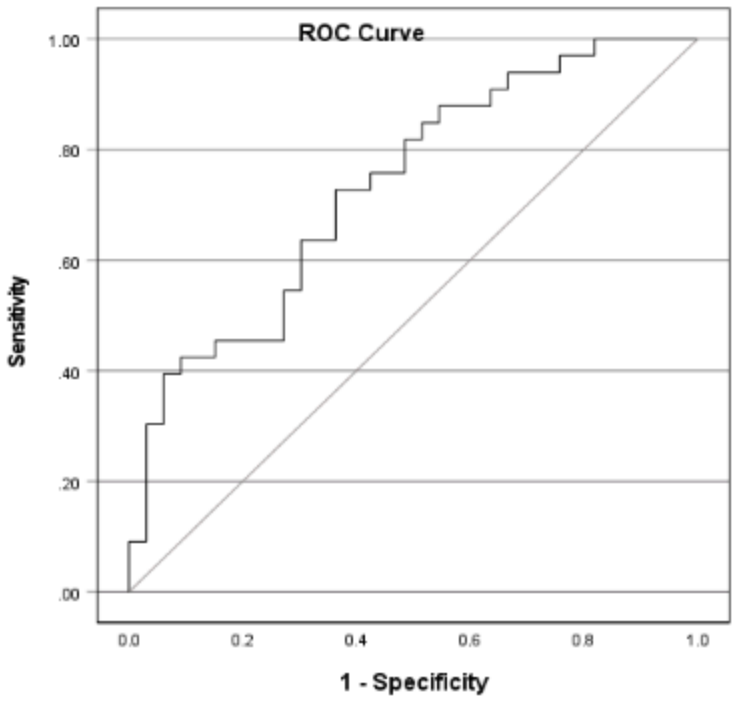


Figure 2

Receiver operating characteristic (ROC) curve analysis evaluating the diagnostic performance of a quantitative optical coherence tomography angiography (OCTA) superficial VDI and determining the optimal cutoff value for differentiating Ocular Surface Squamous Neoplasia (OSSN) from Pterygium, with the best threshold selected to maximize sensitivity and specificity.

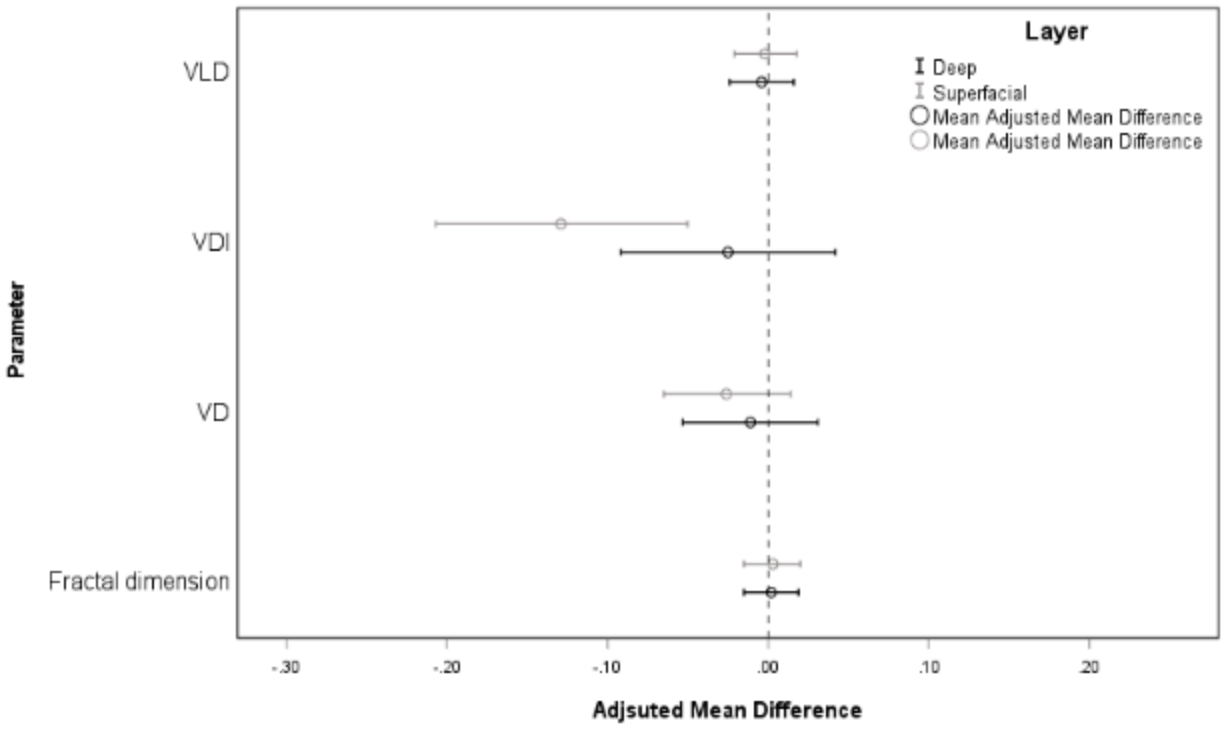


Figure 3

Age- and sex-adjusted differences in quantitative OCTA parameters between pterygium and OSSN. Points represent adjusted mean differences and horizontal bars indicate 95% confidence intervals. The vertical dashed line represents a difference of 0, indicating no between-group difference.

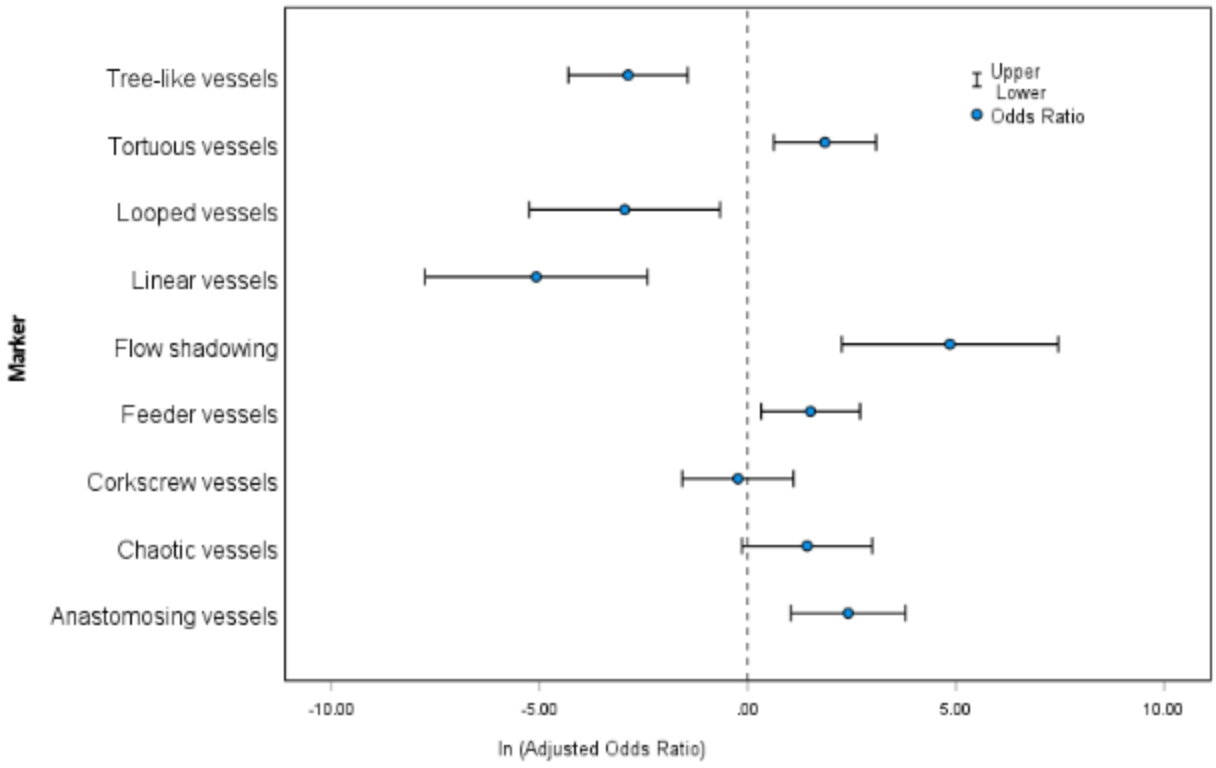


Figure 4

Age- and sex-adjusted odds ratios for qualitative vascular patterns associated with pterygium relative to OSSN. Points represent adjusted odds ratios and horizontal bars indicate 95% confidence intervals. The vertical dashed line represents an odds ratio of 1, indicating no association between lesion type and the vascular pattern.